

## First-Order Torques and Solid-Body Spinning Velocities in Intense Sound Fields\*

T. G. Wang and H. Kanber

*Jet Propulsion Laboratory, California Institute of Technology, Pasadena, California 91103*

and

I. Rudnick†

*University of California, Los Angeles, California 90024*

(Received 29 September 1976)

We report the first observation of first-order nonzero time-averaged torques and solid-body spinning velocities in intense acoustic fields, which occur when the acoustic displacement amplitude exceeds the viscous penetration depth.

Nonzero time-averaged forces, torques, and velocities in intense sound fields have always been associated with second-order nonlinear effects. We have observed a rather striking phenomenon which, for acoustic displacement amplitudes larger than the viscous penetration depth, is a first-order effect. As far as we know, this is the first time that such an effect has been identified.

Consider a rigid rectangular enclosure of dimensions  $l_x$ ,  $l_y$ , and  $l_z$  in the respective Cartesian coordinate directions  $x$ ,  $y$ , and  $z$ , with  $z$  vertical. Let  $l_x = l_y = l$  so that the  $(1, 0, 0)$  and  $(0, 1, 0)$  modes are degenerate. If these two modes are equally excited, and if the origin of coordinates is at the center of the enclosure, then the  $x$  and  $y$  components of the particle velocity,  $v_x$  and  $v_y$  (where  $v_z = 0$ ), will be given by

$$\begin{aligned} v_x &= v_0 \cos(\pi x/l) \cos \omega t, \\ v_y &= v_0 \cos(\pi y/l) \cos(\omega t + \Delta\varphi). \end{aligned} \quad (1)$$

As is well known, the resulting air motion is, in general, elliptical (see, e.g., the Lissajous patterns).

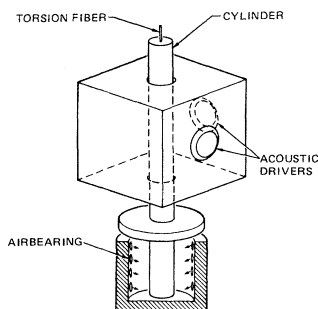


FIG. 1. The experimental apparatus consists of a vertical cylindrical rod, 1 in. in diameter, supported on an air bearing, and passing through a box 4 in.  $\times$  4 in.  $\times$  5 in. with two loudspeakers centered on adjoining 4-in.  $\times$  5-in. vertical sides.

We have focused our attention on the case where the air-particle motion at or near  $x = y = 0$  is circular, i.e., for  $\Delta\varphi = \pi/2$  or  $3\pi/2$ . These two cases differ only in the sense of rotation of the air particles. The linear speed of rotation is  $v_0$ .

Consider a solid cylinder of radius  $r$ , very small compared to  $l$ , free to rotate, with its axis in the  $z$  direction and located at  $x = y = 0$  (see Fig. 1). When surrounded by a gas in which the particles all are executing a circular motion of the same sense with velocity  $v_0$  and radius  $x_0 = v_0/\omega$ , the cylinder will be dragged into rotation also, because of the gas viscosity (to the extent that the quadrupolar scattered acoustic field of the cylinder can be neglected). If the radius  $x_0$  is much less than the viscous penetration depth,  $l_\eta$ , given by  $l_\eta = (2\eta/\rho\omega)^{1/2}$ , where  $\eta$  is the coefficient of viscosity of the gas and  $\rho$  is the gas density, then the rim velocity of rotation of the cylinder is much less than  $v_0$ . This is so because the drag on the cylinder generated by the antiparallel phases of the circular motion of the air particles tends to cancel. In this case, the rim velocity will vary as the product of particle velocity  $v_0$ , and the radius of circulation  $x_0$ , which is second order in  $v_0$ . However, when  $x_0 \geq l_\eta$ , the drag on the cylinder will be dominated by the phase of the air-particle circular motion that is nearer the cylinder surface. In this latter case, the rim velocity of the cylinder can be expected to approach  $v_0$  and it will be first order in  $v_0$ .

Figure 1 is a diagram of the experimental apparatus. It consists of a vertical cylindrical rod, 1 in. in diameter, supported on an air bearing, and passing through a box 4 in.  $\times$  4 in.  $\times$  5 in. which has two loudspeakers centered on adjoining 4-in.  $\times$  5-in. vertical sides. The amplitudes of the  $(1, 0, 0)$  and  $(0, 1, 0)$  modes are set equal and the phase difference of the two modes,  $\theta$  in Eq. (1), can be varied with a phase-shifter. The fre-

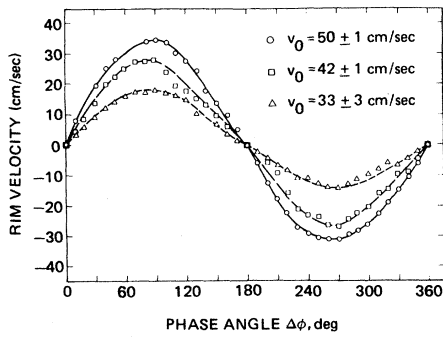


FIG. 2. The rim speed of the cylinder as a function of the phase difference between the  $x$  and  $y$  components of the particle velocity,  $v_0$ , for various values of particle velocity. The points are experimental values. The curves are to guide the eyes and do not represent any theory.

quency of the degenerate acoustic modes is 1.62 kHz and  $l_\eta$  is accordingly  $5 \times 10^{-3}$  cm.

Figure 2 shows the rim speed of the cylinder as a function of the phase difference for various values of  $v_0$ . In this measurement, the weight of the cylinder is supported by air jets rather than by a torsion fiber as shown in Fig. 1; therefore the cylinder is free to rotate. Figure 3 shows the rim speed at  $\theta = 90^\circ$  for a wider range of values of  $v_0$ . It is readily apparent that for large values of  $v_0$ , the rim speed is not far from  $v_0$  and is a linear function of it. ( $x_0 = l_\eta$  when  $v_0 = 52$  cm/sec; it is seen that this is in the linear region.)

We have also measured the torque on the cylinder when it is stationary by suspending it from a torsion fiber and measuring the angular deflection when the sound field is turned on. Figures 4 and 5 show the results as functions of  $\theta$  and  $v_0$ , and

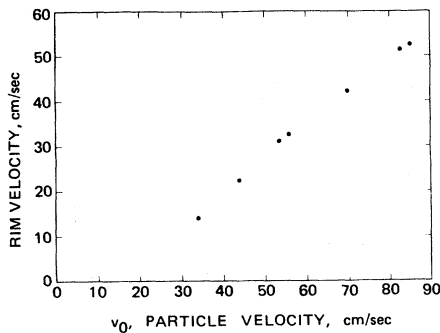


FIG. 3. The rim speed of the cylinder as a function of particle velocity,  $v_0$ , at a phase difference of  $90^\circ$ . The points are experimental values. In the region where particle velocities are higher than 52 cm/sec (where  $x_0 > l_\eta$ ), it is seen that the rim velocity is linearly dependent on the particle velocity.

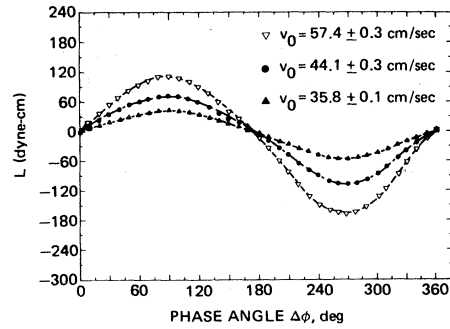


FIG. 4. The acoustic torque as a function of the phase difference between the  $x$  and  $y$  components of the particle velocity,  $v_0$ , for various values of the particle velocity. The points are experimental values. The curves are to guide the eyes and do not represent any theory.

the results parallel those for the rim velocity.

One might expect that circular streaming of the air around the cylinder is responsible, at least partially, for the torque and the spinning of the cylinder, but this is not so. Using smoke streams, we find no evidence of streaming around the cylinder when it is stationary. When it is free to rotate, of course there will be rotation about the axis of the cylinder, but it is the spinning cylinder which creates the circulation and not vice versa.

We have, so far, been unsuccessful in constructing a proper theoretical description of the effects we have presented. This is not surprising, in view of the fact that no one has yet given the exact description (including viscous effects) of the particle motion next to a rigid plate when a sound wave propagates parallel to the plate.<sup>1</sup> Intuitive arguments and approximate treatments<sup>2,3</sup> have served to provide workable descriptions of this

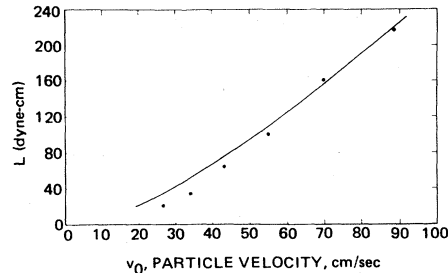


FIG. 5. The acoustic torque as a function of particle velocity,  $v_0$ , at a phase difference of  $90^\circ$ . The points are experimental values. The curve is Eq. (2) of the text. On this curve, in the region where the particle velocities are higher than 52 cm/sec (where  $x_0 > l_\eta$ ), it is seen that the torque is a linear function of the particle velocity.

motion. Our problem is much more difficult, however, given the more complicated nature of the scattering field of a circular cylinder in a plane-wave field.

In the spirit of our earlier discussion, we can go a bit further in understanding our results. One can argue that the torque,  $L$ , on the cylinder of radius  $r$  should be given, approximately, by

$$L = \eta[v_0/l_\eta - v_0/(l_\eta + x_0)]Ar, \quad (2)$$

where  $A$  is the surface area of the cylinder inside the acoustic chamber. The physical ideas which prompt us to write Eq. (2) are as follows: (1) Appreciable motion of the fluid relative to the cylinder can only occur at distances from its surface which are equal to or exceed  $l_\eta$ . (2) Because  $r \gg x_0$ , one can neglect the curvature of the cylinder in obtaining the viscous stress. (3) The gradient in velocity normal to the cylindrical surface can be approximated by the fluid velocity divided by the distance from the surface. (4) If the viscous force per unit area during the positive phase of the orbital fluid motion is  $\eta v_0/l_\eta$ , then, in this approximation, it is  $\eta v_0/(l_\eta + x_0)$  during the opposite phase of the motion. Equation (2) is the curve plotted in Fig. 5 and it is clear that a task for the theory is to provide a torque which in some approximation yields Eq. (2).

One more point should be made. Suppose that we consider a circular disk of infinitesimal thick-

ness, lying in the  $x$ - $y$  plane. Then, since our understanding of the origin of the first-order behavior involves interactions at the rim, where displacements greater than  $l_\eta$  can take the air particles out of the viscous layer, we would expect that the torques and velocities on such a disk would be second order. We have made quantitative observations on such a disk and indeed this is the case.

It is a pleasure to acknowledge the value of discussions with Dr. S. Putterman of the University of California at Los Angeles, and we are indebted to Dr. P. Mason of the Jet Propulsion Laboratory for his critical reading of the manuscript. The authors also wish to thank Mr. E. Olli of the Jet Propulsion Laboratory and Mr. S. Adams of the University of California at Los Angeles for their excellent help.

---

\*Work sponsored by the National Aeronautics and Space Administration under Contract No. NAS 7-100.  
 †Work partially supported by Nonr Contract No. N000-14-75-C-0246.

<sup>1</sup>S. Putterman, private communication.

<sup>2</sup>I. Todhunter, in *A History of the Theory of Elasticity and of the Strength of Materials*, edited by K. Pearson (Cambridge Univ. Press, Cambridge, England, 1960), Vol. II.

<sup>3</sup>Lord Rayleigh, *The Theory of Sound* (Dover, New York, 1945), Vol. II.

---

## Generation of 0.2-TW Proton Pulses

J. Golden, C. A. Kapetanakis, S. J. Marsh,\* and S. J. Stephanakis  
*Naval Research Laboratory, Washington, D. C. 20375*

(Received 22 October 1976)

Results are reported on the generation of MeV, pulsed ion beams at a peak power level in excess of  $2 \times 10^{11}$  W that have an angular divergence of about  $3^\circ$ - $4^\circ$ . Such beams can be used in the formation of field-reversing proton rings.

Presently there are several schemes<sup>1-8</sup> available to produce intense, pulsed ion beams. An important motive for the generation of such beams is their potential application to the formation of field-reversing ion layers and rings.<sup>9-11</sup> The results of the present experiment demonstrate unequivocally that existing pulsed-power technology can provide sufficient ions, in a single pulse, which, if converted into a ring or layer, could produce field reversal.<sup>12</sup>

Briefly, in this experiment we have produced

hollow, pulsed proton beams in the energy range between 0.6 and 1.2 MeV and peak proton current in excess of 200 kA using a low-inductance, coaxial reflex triode. For the best-quality beam produced the angular divergence is between  $3^\circ$  and  $4^\circ$ .

A schematic of the experiment is shown in Fig. 1. The 0.6-1.2-MV positive pulse (total energy  $\sim 30$ - $40$  kJ) from the GAMBLE II generator<sup>13</sup> is applied to the anode, which is constructed from solid  $12.5\text{-}\mu\text{m}$ -thick polyethylene film mounted be-